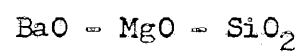


SOLID STATE RELATIONSHIPS IN THE SYSTEM



by

H. Erman Tulgar

ProQuest Number: 10795642

All rights reserved

INFORMATION TO ALL USERS

The quality of this reproduction is dependent upon the quality of the copy submitted.

In the unlikely event that the author did not send a complete manuscript and there are missing pages, these will be noted. Also, if material had to be removed, a note will indicate the deletion.



ProQuest 10795642

Published by ProQuest LLC (2018). Copyright of the Dissertation is held by the Author.


All rights reserved.

This work is protected against unauthorized copying under Title 17, United States Code
Microform Edition © ProQuest LLC.

ProQuest LLC.
789 East Eisenhower Parkway
P.O. Box 1346
Ann Arbor, MI 48106 – 1346

A thesis respectfully submitted to the Faculty and the Board of Trustees of the Colorado School of Mines in partial fulfillment of the requirements for the degree of Master of Science in Metallurgical Engineering.

Signed:



H. Erman Tulgar

Approved:


P. G. Herold
Thesis Advisor

Golden, Colorado

Date: May 12, 1965


A. W. Schlechten, Head
Department of
Metallurgical Engineering

ABSTRACT

Compositions in the ternary system $\text{BaO} - \text{MgO} - \text{SiO}_2$ were made from A.R. BaCO_3 , U.S.P. MgCO_3 and ground quartz. Spectrographic analysis showed that these compounds were relatively pure, containing very small amounts of Mg, Si and Ca in all three. Over one hundred samples were made in the form of tetrahedrons and fired at 50°C less than the temperature at which the glassy phase formed and held at this temperature to produce equilibrium conditions. These samples were analyzed by X-Ray diffraction technique and the results represented on a solid-state phase diagram which resulted in twenty-one Alkemade lines forming eleven Alkemade triangles. Two intermediate compounds, $\text{BaO}\cdot 2\text{MgO}\cdot 2\text{SiO}_2$ and $\text{BaO}\cdot \text{MgO}\cdot 2\text{SiO}_2$ were found to exist in the system. Other compounds reported in the literature which were found to be non-existent are $\text{BaO}\cdot 3\text{MgO}\cdot 2\text{SiO}_2$, $3\text{BaO}\cdot \text{MgO}\cdot 2\text{SiO}_2$ and $2\text{BaO}\cdot \text{MgO}\cdot 2\text{SiO}_2$.

TABLE OF CONTENTS

	Page
ABSTRACT	iii
TABLE OF CONTENTS	iv
LIST OF FIGURES	vi
LIST OF TABLES	vii
ACKNOWLEDGMENTS	viii
INTRODUCTION	1
Approach used in this work	2
REVIEW OF LITERATURE	4
The two component system $MgO - SiO_2$	4
The two component system $BaO - MgO$	6
The two component system $BaO - SiO_2$	8
The three component system $BaO - MgO - SiO_2$ (according to Klasens)	8
The three component system $BaO - MgO - SiO_2$ (according to Nadachowski and Grylecki)	10

	Page
EXPERIMENTAL MATERIALS AND PROCEDURE	13
Materials used	13
Preparation of samples	15
Heat treatment	15
Methods of analysis	16
DATA AND DISCUSSION	18
BaO·MgO·SiO ₂ and BaO·2MgO·2SiO ₂ ternary compounds	20
Questionable intermediate compounds	21
The determination of the true Alkemade lines	23
Solid solution	28
Suggestions for further study	32
SUMMARY	33
CONCLUSIONS	35
APPENDIX A	36
BIBLIOGRAPHY	57
VITA	59

LIST OF FIGURES

Figure	Page
1. The two phase system $MgO - SiO_2$	5
2. Liquidus curve of the system $BaO - MgO$	7
3. The two phase system $BaO - SiO_2$	9
4. Phase relations between $BaO - MgO - SiO_2$ according to Klasens	11
5. Phase relations between $2CaO \cdot SiO_2 - 2BaO \cdot SiO_2 -$ $2MgO \cdot SiO_2$ according to Nadachowski and Grylecki ..	12
6. $BaO - MgO - SiO_2$ phase diagram according to Klasens + data from Table IV	24
7. Phase relations between $BaO - MgO - SiO_2$ developed from experimental data	25
8. Comparison of X-Ray diffraction patterns for composition between EMS and BS	26
9. Comparison of X-Ray diffraction patterns for composition in the solid solution region	31

LIST OF TABLES

Table	Page
I. One and two component compounds in the three component system $\text{BaO} - \text{MgO} - \text{SiO}_2$	19
II. Intermediate compounds $\text{BaO} \cdot 2\text{MgO} \cdot 2\text{SiO}_2$, $\text{BaO} \cdot 3\text{MgO} \cdot 2\text{SiO}_2$, and $\text{BaO} \cdot \text{MgO} \cdot \text{SiO}_2$	20
III. Questionable intermediate compounds	21
IV. Data for developing Alkemade lines in questionable area ..	22
V. Data for developing Alkemade lines	27
VI. Data for compounds in solid solution area	29

ACKNOWLEDGMENTS

The author takes this opportunity to express his gratitude and appreciation to Dr. P. G. Herold for guidance and encouragement during the initiation and progress of this investigation.

Also acknowledgment is given to the Agency for International Development, United States Department of State (AID) and the Turkish Government for financial support of the author in his work toward the Master of Science degree.

INTRODUCTION

Since the Metallurgical Industry has been progressively changing its processing so as to use higher and higher temperatures, the Refractory manufacturer has had to search for higher temperature refractories.

One of the recent advances in metallurgical practice has been the change from the use of the open hearth to the oxygen retort in the conversion of pig iron to steel. This has made it necessary to investigate and use a refractory composed essentially of the alkaline earth oxide, magnesia. Since this type of compound is characterized by a high melting point, the other alkaline earth oxides are also being investigated commercially. Thus the whole area of combinations between magnesia (MgO), lime (CaO), barium oxide (BaO), alumina (Al₂O₃), silica (SiO₂), and the major contaminant ferrous iron oxide (FeO), is being considered by the metallurgist and the ceramist.

As a preparatory step in the investigation of any refractory system, the relationships between the compounds generated at high temperatures is first considered. It is apparent that the phase diagrams between the compounds mentioned should be available to the research

worker in his search for better refractories.

From the phase relationship standpoint, not much is known about the combinations of barium oxide with the other oxides mentioned. The present investigation of the solid state reactions between BaO, MgO, and SiO₂ was initiated to correct this situation.

Small amounts of barium oxide are often used in various ceramic body combinations. Therefore, the solid state phase diagram resulting from the present study is also of general interest to Ceramic Engineers.

Approach used in this work

In this work, compositions were selected which occur half way between the known compositions which were assumed to be compatible. Since such a composition would then be on an Alkemade line, there would only be two crystalline compounds present under equilibrium conditions. If the selected composition does not lie on a line between two compatible compounds, three crystalline materials generally will be present in the sample. In rare cases it could be possible that such a composition would occur on another Alkemade line. Occasionally compositions were selected to occur inside an Alkemade triangle so as to check the presence of three compatible compounds. If more than three compounds are present in any heat treated mixture, equilibrium was not obtained and the mixture needs to be heated longer and/or at a higher temperature. All identification of crystalline compounds present in the heat treated samples were made by X-Ray diffraction methods. This gives a permanent

record as compared to optical-constants measurements.

Many compounds are capable of becoming luminescent under electron bombardment when the compound has been activated by incorporating a small amount of impurity into the crystal structure. This characteristic can be used to identify compounds in an unknown phase system, however the method was not used in the present work. This method would have been useful if a new compound had been determined in the investigation of the BaO - MgO - SiO₂ system.

REVIEW OF LITERATURE

The two component system MgO-SiO_2 . This system was originally worked out by Bowen and Anderson⁽¹⁾ and modified by Grieg⁽²⁾. They showed that the two intermediate compounds, forsterite ($2\text{MgO}\cdot\text{SiO}_2$) and clinoenstatite ($\text{MgO}\cdot\text{SiO}_2$) are formed. The diagram of this system is shown in Figure 1. There are a total of six crystalline compounds in the system; these being besides forsterite and clinoenstatite, periclase (MgO), α -quartz (SiO_2), α -Cristobalite (SiO_2), and α -tridymite (SiO_2). Periclase crystallizes in the cubic face centered system similar to NaCl , and has a unit cell dimension of $a_0 = 4.213 \text{ A.U.}$ ⁽³⁾ The X-Ray diffraction pattern and all subsequent patterns which are known, were obtained from the A.S.T.M.⁽⁴⁾ file of standard patterns. They are listed in Appendix A.

-
- (1) Bowen, N. L. and Anderson, O. "The binary system $\text{MgO} - \text{SiO}_2$." *Am. J. Sci.*, (4), 37, 488 (1914).
 (2) Grieg, J. W. "Immiscibility in silicate melts." *Am. J. Sci.* (5) 13, 15, 133-54 (1927).
 (3) Swanson and Tatge. "Standard X-Ray diffraction powder patterns." NBS Circular 539, I, 37-8 (1962).
 (4) Index to the X-Ray Powder data file, ASTM, Special Technical Publication 48-2 (1962).

MgO-SiO₂

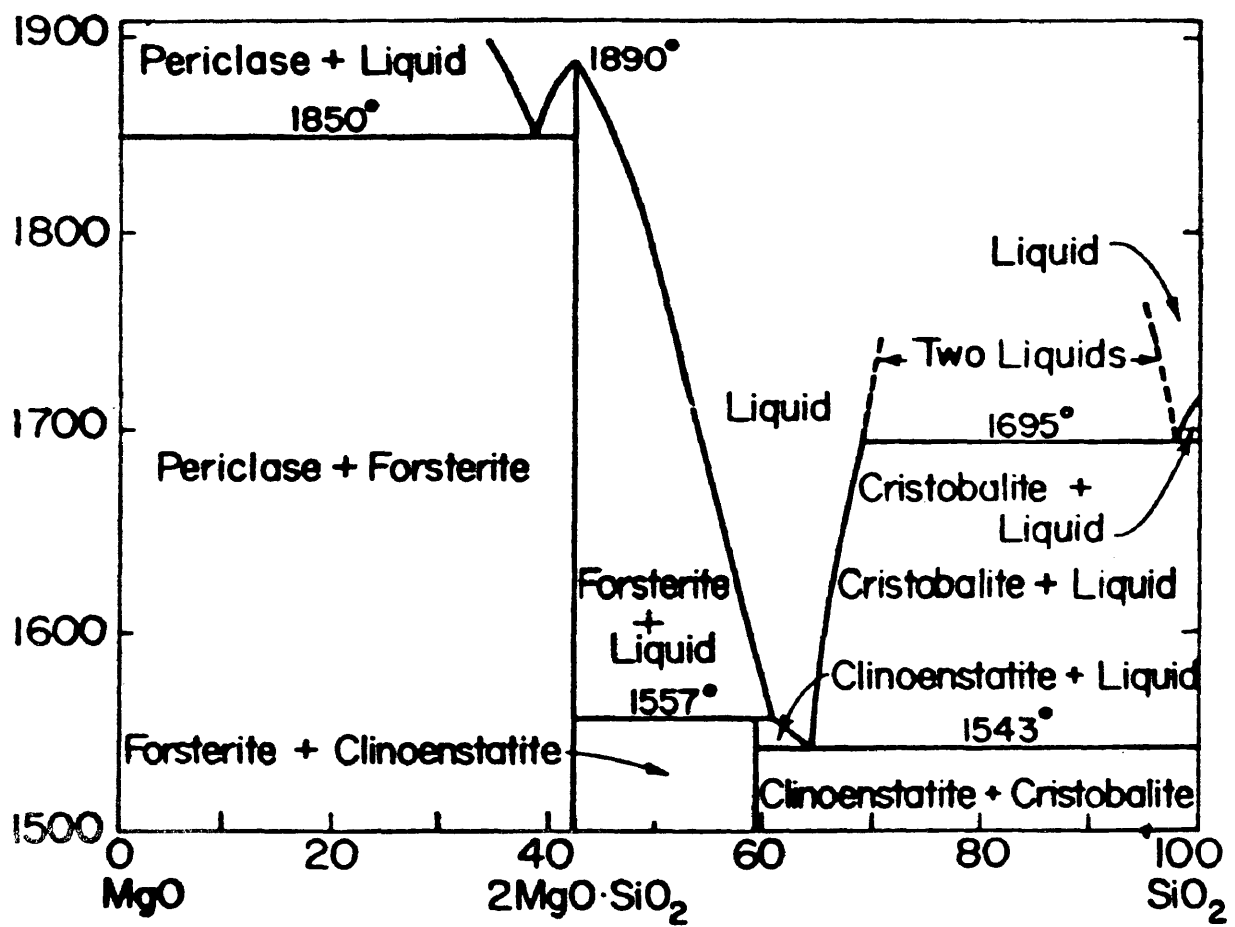


Figure 1. The two phase system MgO-SiO₂.

Forsterite ($2\text{MgO}\cdot\text{SiO}_2$) crystallizes in the orthorhombic system, having a unit cell size of $a_0 = 4.76$ A.U., $b_0 = 10.20$ A.U., and $c_0 = 5.99$ A.U. (5). Clinoenstatite ($\text{MgO}\cdot\text{SiO}_2$) has not been investigated as far as the crystal structure is concerned. The three crystalline room temperature modifications of silica are α -quartz, α -cristobalite, and α -tridymite, the first two of which crystallize in the hexagonal system, while the latter crystallizes in the rhombohedral system. Their unit cell dimensions are:

Crystal	a_0	b_0	c_0
α -quartz	4.913 A.U.		5.405 A.U. (6)
α -cristobalite	*		
α -tridymite	9.88 A.U.	17.1 A.U.	16.3 A.U. (7)

*The structure of α -cristobalite has not been completed.

The two component system $\text{BaO} - \text{MgO}$ has been partially worked out by Wartenberg and Prophet (8) and is shown in Figure 2. This diagram indicates that even though the data are incomplete, no intermediate compounds exist in the system, and there is no solid solution. Barium oxide (BaO)

-
- (5) Bragg and Brown, Z. Krist 63, 538 (1926).
 (6) Swanson and Fuyat, Standard X-Ray diffraction patterns, NBS Circular 539, III, 24-6 (1954).
 (7) Clark, C. B., "X-Ray diffraction data for compounds in the system CaO-MgO-SiO_2 ." J. Am. Ceram. Soc. 29, 25 (1946).
 (8) Wartenberg, H. von and Prophet, E. "Schmelzdiagramme höchstfeuerfester Oxyde, V. Systeme mit MgO ." partV, Z. anorg. U. Allgem. chem. 208, 378 (1932).

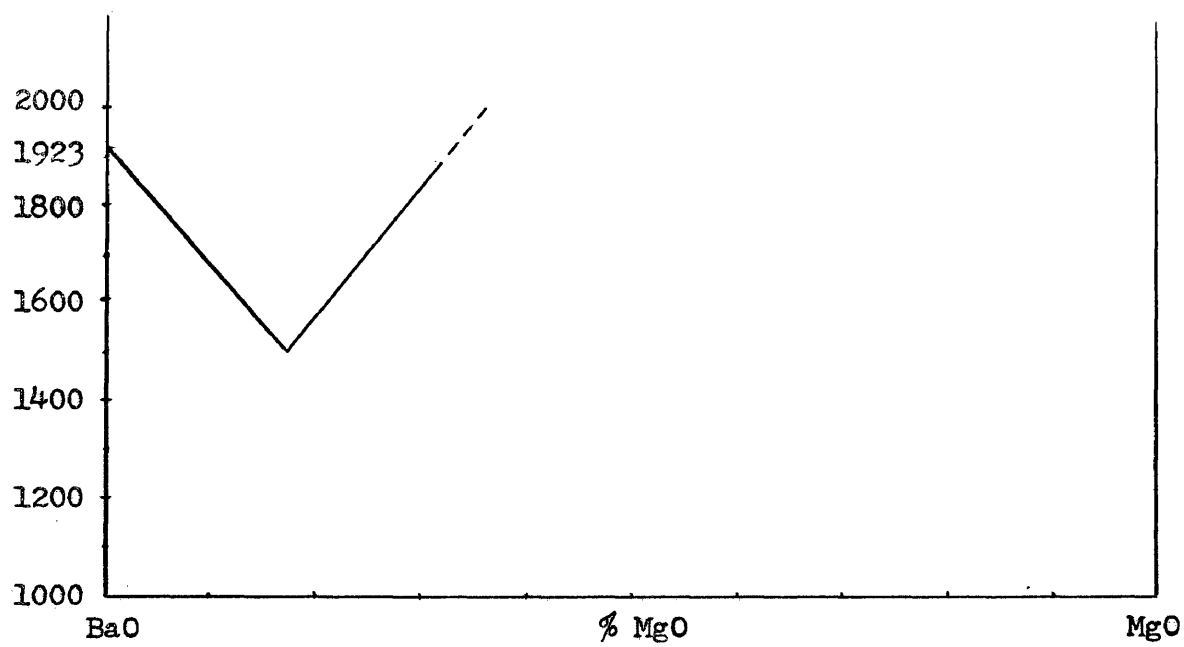


Figure 2. Liquidus curve of the system BaO - MgO.

crystallizes in the face centered cubic configuration similarly to NaCl and has a unit cell size of 5.50 A. U. (9).

The two component system BaO - SiO₂ has been investigated by Eskola (10) and modified by Grieg (11). The diagram is shown in Figure 3, and indicates the presence of four intermediate compounds; 2BaO·SiO₂, BaO·SiO₂, 2 BaO·3SiO₂ and BaO·2SiO₂ (Sanbornite). The unit cell dimensions of these compounds and their crystal habit have not been identified, however, the X-Ray diffraction patterns have been published. The phase diagram shows a composition range of solid solution between 2BaO·3SiO₂ and BaO·2SiO₂.

Portions of the three component system BaO - MgO - SiO₂ have been investigated, but there is much controversy over the intermediate compounds present and the relationships between them under equilibrium conditions. Klasens and co-workers (12) in their work on luminescent materials investigated this system and identified the compounds BaO·MgO·SiO₂, 3 BaO·MgO·2SiO₂, 2BaO·MgO·2SiO₂, and BaO·2MgO·2SiO₂. These materials were activated with one mole percent Pb and gave characteristic blue cathodoluminescent emission. They reported the X-Ray

-
- (9) Wyckoff, "The crystal structures of the compounds RX" The Structure of crystals page 224 (1963).
- (10) Eskola, P. "The silicates of strontium and barium" Am. J. Sci. 5th ser. 4, 345 (1922).
- (11) Grieg, J. W. "The system BaO - SiO₂" Am. J. Sci., 5th ser. 13, 27 (1927)
- (12) Klasens, H. A., Hoekstra, A. H., and Cox, A. P. M. "Ultra-violet fluorescence of some Ternary Silicates Activated with Lead." J. Electrochem. Soc. 104, 93-99 (1957).

BaO-SiO₂

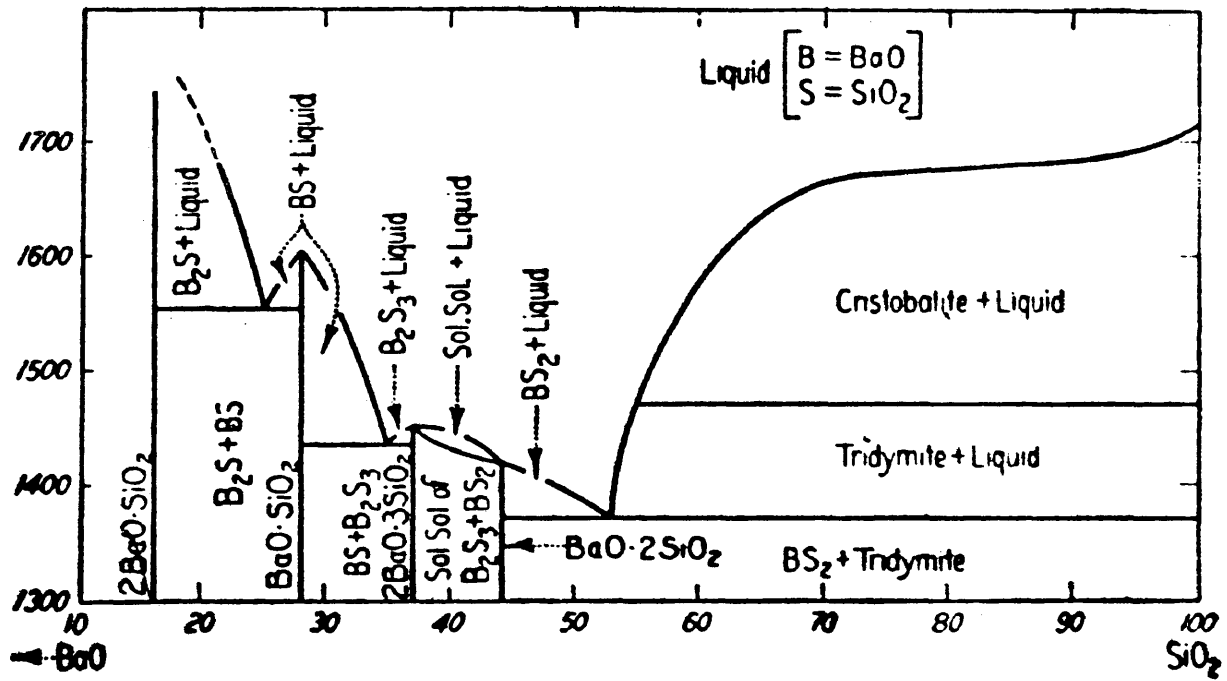


Figure 3. The two phase system BaO - SiO₂.

diffraction patterns for these compounds which are reproduced in Appendix A. Figure 4 illustrates the diagram which they published and shows the relationships between the four compounds which they reported.

Nadachowski and Grylecki⁽¹³⁾ worked with mixtures on the plane $2\text{BaO}\cdot\text{SiO}_2 - 2\text{CaO}\cdot\text{SiO}_2 - 2\text{MgO}\cdot\text{SiO}_2$. They report two new compounds $\text{BaO}\cdot 3\text{MgO}\cdot 2\text{SiO}_2$ and $\text{BaO}\cdot\text{MgO}\cdot\text{SiO}_2$, and give the X-Ray diffraction patterns which are reproduced in Appendix A. The triaxial diagram that they developed and which is actually a plane through the four component system $\text{BaO} - \text{CaO} - \text{MgO} - \text{SiO}_2$ is shown in Figure 5. The X-Ray diffraction pattern which they report for $\text{BaO}\cdot\text{MgO}\cdot\text{SiO}_2$ is somewhat different from the one reported by Klasens, so it is reproduced in Appendix A, as is the pattern for $\text{BaO}\cdot 3\text{MgO}\cdot 2\text{SiO}_2$.

Yasuno⁽¹⁴⁾ worked in the high silica part of the $\text{BaO} - \text{MgO} - \text{SiO}_2$ system bounded by $\text{BaO}\cdot 2\text{SiO}_2$, SiO_2 , and $\text{MgO}\cdot 2\text{SiO}_2$. Therefore, he did not encounter any of the intermediate compounds in the system.

Turner⁽¹⁵⁾ determined the approximate composition of the lowest fusing mixture in the $\text{BaO} - \text{MgO} - \text{SiO}_2$ system by means of the cone fusion technique. No attempt was made to identify the crystalline compounds developed. The lowest melting point mixture was reported as 46% $\text{BaO} + 8\% \text{MgO} + 46\% \text{SiO}_2$, fusing at 1115°C .

- (13) Nadachowski, F. and Grylecki, M. "Phasen - Gleichgewichte im System $2\text{BaO}\cdot\text{SiO}_2 - 2\text{CaO}\cdot\text{SiO}_2 - 2\text{MgO}\cdot\text{SiO}_2$." *Silikattechn* 10, 77-80 (1959).
- (14) Yasuno, F. "Equilibrium Diagram of the area Sanbornite - Forsterite - Silica in the ternary System of $\text{MgO} - \text{BaO} - \text{SiO}_2$. Studies on the Deterioration Phenomenon of Steatite Bodies, III." *J. Cer. Assoc. Japan* 67, 403-19 (1959).
- (15) Turner, C. H. "Approximate Composition of the lowest fusing mixture of Barium Oxide, Magnesium Oxide, and Silica." *J. Amer. Cer. Soc.* 17, 14-15 (1934).

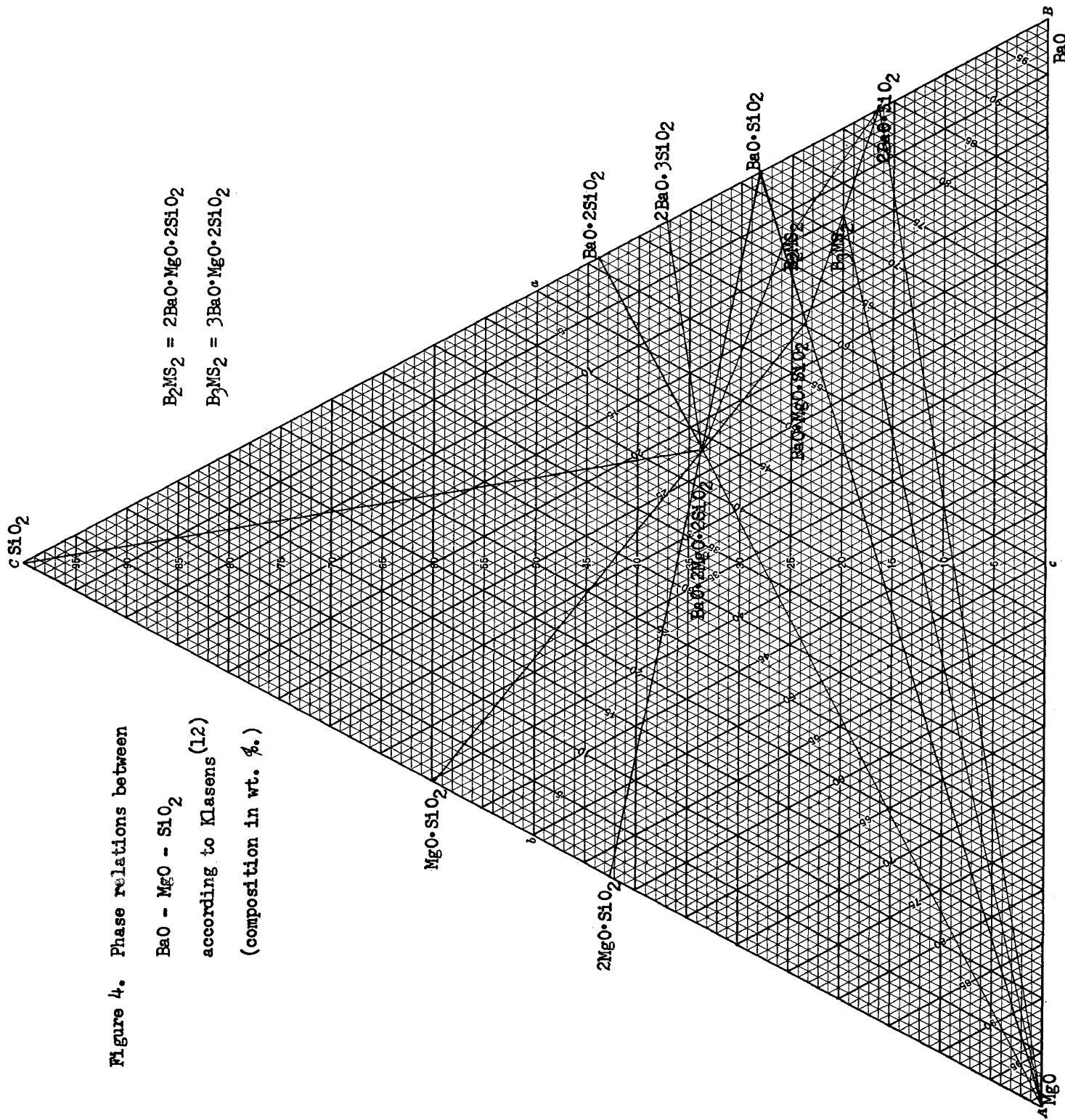


Figure 4. Phase relations between BaO - MgO - SiO₂ according to Klasens (12) (composition in wt. %.)

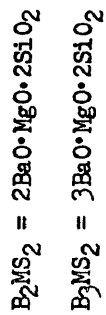
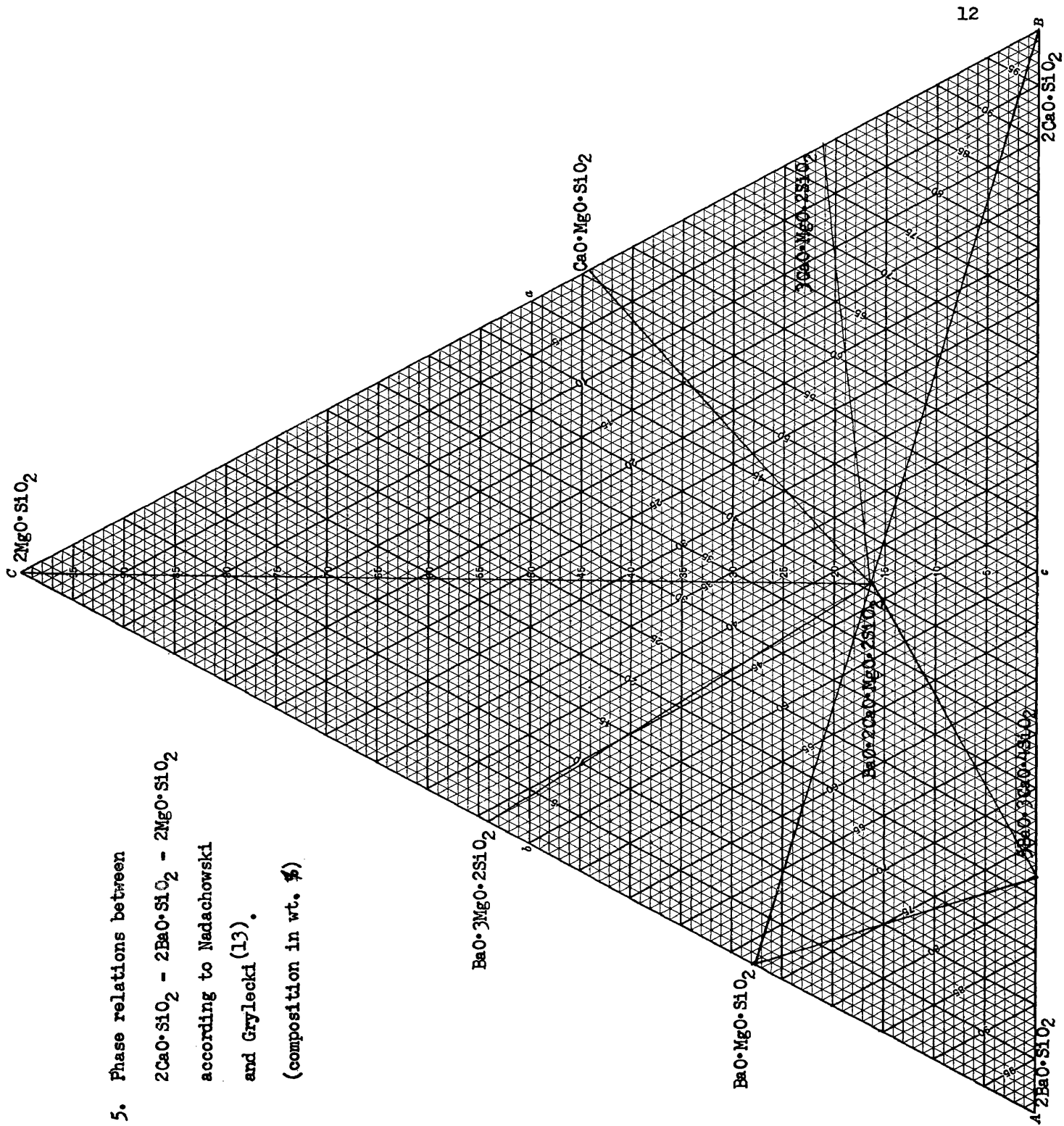


Figure 5. Phase relations between
 $2CaO \cdot SiO_2 - 2BaO \cdot SiO_2 - 2MgO \cdot SiO_2$
 according to Nadachowski
 and Grylecki (13).
 (composition in wt. %)



EXPERIMENTAL MATERIALS AND PROCEDURE

The materials used in this work are barium carbonate as the source of barium oxide, magnesium carbonate as the source of magnesium oxide and 200 mesh crushed quartz as the source of silica. The barium carbonate was obtained from J. T. Baker Co. as the Analytical Reagent, and a spectroscopic analysis was made. The results show that the principal impurities are as follows:

Mg

Si

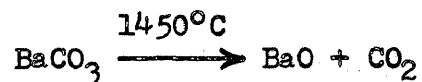
Ca

Sr

Pb

Since barium carbonate loses its carbon dioxide at 1450°C , under atmospheric pressure, a sample was heated to 1500°C . The ignition loss was equal to the theoretical amount; that is, 22.3% which indicates that there was little or no barium hydroxide or other decomposable compounds present in the starting material.

The reaction upon heating is:



An X-Ray diffraction pattern was made of the starting material, barium carbonate, and of the heated material, barium oxide. In each case no lines other than those attributed to the carbonate or the oxide were found on the pattern.

The magnesium carbonate was obtained from Matheson, Coleman and Bell Co. as their U.S. P. light powder. A spectrographic analysis was made and showed the following principal impurities:

Si

Ca

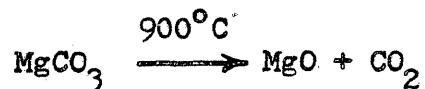
Mn

Mo

Pb

Magnesium carbonate loses its carbon dioxide at 900°C at atmospheric pressure, so a sample was heated to 1000°C . Again the ignition loss was measured to be the theoretical amount being 52.2%.

An X-Ray pattern was made of the magnesium carbonate and of the magnesium oxide and no other lines were formed on the pattern. The reaction upon heating is:



The minus 200 mesh quartz was obtained from the Ottawa Silica Co. A sample was heated to 1000°C and showed zero ignition loss. This

indicates that no carbonate, hydrates, or clay was present in the original material. The X-Ray diffraction pattern of the original raw material showed no lines which could not be attributed to quartz.

A spectrographic analysis was made which showed the following impurities:

Mg

Ba

Cu

Mn

Mo

Compositions which were prepared in the system investigated are designated on an oxide content basis. Therefore, the weighed batch was calculated from the ignition losses as reported above for the three materials. Calculations were carried out to ± 0.01 percent. A ten gram sample was made in every case and weighed on a chemical balance to ± 0.001 grams. The samples were well mixed in the dry state by means of a mortar and pestle. They were then mixed with a 10% dextrin-water solution used as a binder, and small tetrahedrons formed which were 1.1" tall by 0.35" at the base.

The selected batch compositions were mounted on a fire clay brick by sticking the cones to the brick with pure Georgia kaolin slip and firing to a sufficiently high temperature to determine the fusion temperature of each mixture. The firings were made in either a gas fired furnace or a silicon carbide resistance furnace depending on the

ultimate temperature required. The electric furnace has a maximum temperature limit of 1370°C while the gas fired furnace is limited to 1760°C . After the fusion temperature of a mixture was determined by observing the deformation of the tetrahedron, another sample of the same composition was fired to a temperature about 50°C below the deformation temperature and held for at least two hours to obtain equilibrium conditions. The tetrahedrons were quenched by natural cooling of the furnace, removed from the furnace and ground to a fine grained powder with a corundum mortar and pestle.

No chemical analyses were made on the fired materials, but they were held in a dessicator until the X-Ray diffraction pattern was made.

Methods of analysis

Each sample which had been held at a high temperature to obtain equilibrium was subjected to X-Ray diffraction analysis in order to identify the crystalline compounds which had been formed. Both film and diffractometer technique were used. Since the diffractometer method gives a paper graph of the 2θ angle versus intensity of diffraction, most of the compositions were examined in this way. The Debye film technique was used when extreme accuracy was desired in determining the position of the diffracted line. The basic principle underlying the identification of materials by X-Ray diffraction methods is that each crystalline substance gives a characteristic and unique X-Ray diffraction pattern which are superimposed when the

sample is composed of a mixture of crystals.

It is best not to have too many individual crystals in the sample as superimposed lines become very difficult to identify and assign to the proper crystal type.

The diffractometer used in this investigation was the Norelco 170° rotating head and the copper target tube which was operated at 35KV and 25ma. The resulting radiation was filtered by Ni foil so that $K\alpha$ radiation X-Rays only are used. The diffractometer is allowed to run between $2\theta = 7^\circ$ to 67° as this was sufficient to scan all the intense characteristic peaks of the compounds encountered.

The Debye method was carried on the same way except that a 10 cm. diameter camera, and photographic film were used. After development of the film, the d-value of each line was calculated from measurements of the positions of the lines on the film.

When it was apparent from the X-Ray diffraction pattern that solid state equilibrium had not been established, the fired sample was reground, shaped into a tetrahedron and refired for a longer time at the same temperature as used previously, to promote combination and crystallization of the materials.

DATA AND DISCUSSION

As a start into determining the compatibility of crystalline compounds present in the $\text{BaO} - \text{MgO} - \text{SiO}_2$ system, all the known two component compounds were prepared from the raw materials, fired, and X-Ray diffraction patterns made. In each case the compound was identified by comparing with the standard ASTM pattern. No extra lines generated by impurities or other compounds were observed. The following Table shows the compositions made and the results obtained:

Table I

One and Two Component Compounds in the Three Component
System BaO - MgO - SiO₂

Crystalline compound ex- pected	Compo- sition No.	% Composition			Firing Tempe- rature	X-Ray identi- fication
		BaO	MgO	SiO ₂		
B	1	100	0	0	1500°C	B
M	2	0	100	0	1000°C	M
S	3	0	0	100	1000°C	S
BS ₂	4	56	0	44	1370°C	BS ₂
B ₂ S ₃	5	62.96	0	37.04	1400°C	B ₂ S ₃
BS	6	71.84	0	28.16	1500°C	BS
B ₂ S	7	83.61	0	16.39	1475°C	B ₂ S
MS	8	0	40.20	59.80	1475°C	MS
M ₂ S	9	0	57.30	42.70	1500°C	M ₂ S

Where B = BaO

M = MgO

S = SiO₂, and the subscript numbers mean number of moles
of the indicated oxide.

Next, the compounds EM_2S_2 and EMS were made and identified as being unique materials. These were made since there seems to be general agreement in the literature that they exist. The following Table gives the data concerning them:

Table II

Intermediate Compounds EM_2S_2 , EM_3S_2 and EMS

Crystalline compound expected	Composition No.	% Composition			Firing Temperature	X-Ray identification
		BaO	MgO	SiO ₂		
EM_2S_2	46	43.30	22.70	33.93	1425°C	EM_2S_2
EMS	13	60.43	15.88	23.69	1425°C	EMS
EM_3S_2	12	38.87	30.66	30.47	1425°C	$EM_2S_2 + M$

Klasens identified the compound EM_2S_2 and published the X-Ray diffraction pattern as listed in Appendix A. The pattern which was obtained in the present work was similar in every respect to Klasens' pattern except that a strong line (10% of the strongest line) is present at $d = 6.32$ A. U. ($2\theta = 14.00$). The reason that Klasens' pattern does not show this line is that he shows no data below $d = 4.60$ and, therefore, probably he missed this line.

Nadachowski and Grylecki do not report the compound EM_2S_2 but do report a new compound " EM_3S_2 ". The pattern which they report for this new compound is the same as Klasens' " EM_2S_2 " except that they report a new line, $d = 6.49$ A. U. The pattern for EM_3S_2 is given in Appendix A,

and a comparison with Klasens' " EM_2S_2 " shows that the lines for the EM_3S_2 are all shifted to higher d-values. Data which is presented later in this report will show that the composition EM_3S_2 does not exist but is actually a mixture of $EM_2S_2 + M$.

The compound EMS which was first reported by Klasens was also reported by the Russians and is produced in the present work. The three X-Ray diffraction patterns are similar so that there is no difference of opinion with respect to the compound EMS.

Klasens reports the existence of two more compounds, B_2MS_2 and B_3MS_2 . These compounds were not reported by the Russians and the present work proves that they do not exist. The following Table gives the data concerning these two compounds when produced in the laboratory:

Table III

Crystalline compound expected	Composition No.	Questionable Intermediate Compounds % Composition			Firing Temperature	X-Ray Identification
		BaO	MgO	SiO ₂		
B_2MS_2	45	65.64	8.63	25.73	1425°C	EMS + BS
B_3MS_2	44	74.13	6.51	19.36	1425°C	EMS + B ₂ S

Later it will be shown that these two compounds B_2MS_2 and B_3MS_2 actually occur on the Alkemade lines between EMS and BS and EMS and B₂S respectively.

Table IV

Data for Developing Alkemade Lines in Questionable Areas.

Compo- sition No.	% Composition			Firing Tempe- rature	Compounds present =	
	BaO	MgO	SiO ₂		According to Klasens	Actually present
52	63.04	12.25	24.71	1425°C	B ₂ MS ₂ + BMS	BMS + BS
53	68.74	4.32	26.94	"	" + BS	" + "
50	69.89	7.57	22.54	1290°C	" + B ₃ MS ₂	" + " + B ₂ S
49	72.99	3.25	23.76	"	" + BS + B ₂ S	" + " + "
44	74.13	6.51	19.36	1425°C	B ₃ MS ₂	" + B ₂ S
48	67.28	11.20	21.52	"	" + EMS	" + "
47	78.87	3.26	17.87	"	" + B ₂ S	" + "
91	54.47	15.70	29.83	1300°C	EM ₂ S ₂ + B ₂ MS ₂	" + EM ₂ S ₂ + BS ₂
45	65.64	8.63	25.73	1425°C	B ₂ MS ₂	" + BS
85	69.44	15.33	15.23	"	B ₃ MS ₂ + B ₂ S + M	" + B ₂ S + M
101	57.22	10.74	32.04	1300°C	EM ₂ S ₂ + BS + B ₂ S ₃	" + EM ₂ S ₂ + BS ₂
55	64.30	4.32	31.38	1260°C	" + " + "	" + BS + B ₂ S ₃

It is necessary to try to determine why Klasens made the mistake of identifying B₂MS₂ and B₃MS₂ as new compounds. The compositions in Table IV were then made to try to clarify this area of the diagram.

From the data in Table IV and the phase diagram according to Klasens shown as Figure 4, a diagram was constructed shown in Figure 6. The data from Table IV were entered on Figure 6 and immediately indicate

that Klasens' Alkemade lines:

- | | |
|------------------------|---------------------------|
| a) M to B_3MS_2 | f) B_2MS_2 to B_3MS_2 |
| b) B_3MS_2 to B_2S | g) " to B_2S |
| c) " to EMS | h) EM_2S_2 to BS |
| d) B_2MS_2 to " | i) " to B_2S_3 |
| e) " to BS | j) " to B_2MS_2 |

are not true Alkemade lines. According to the experimental data in Table IV, the true Alkemade lines in this area are shown on Figure 7 as:

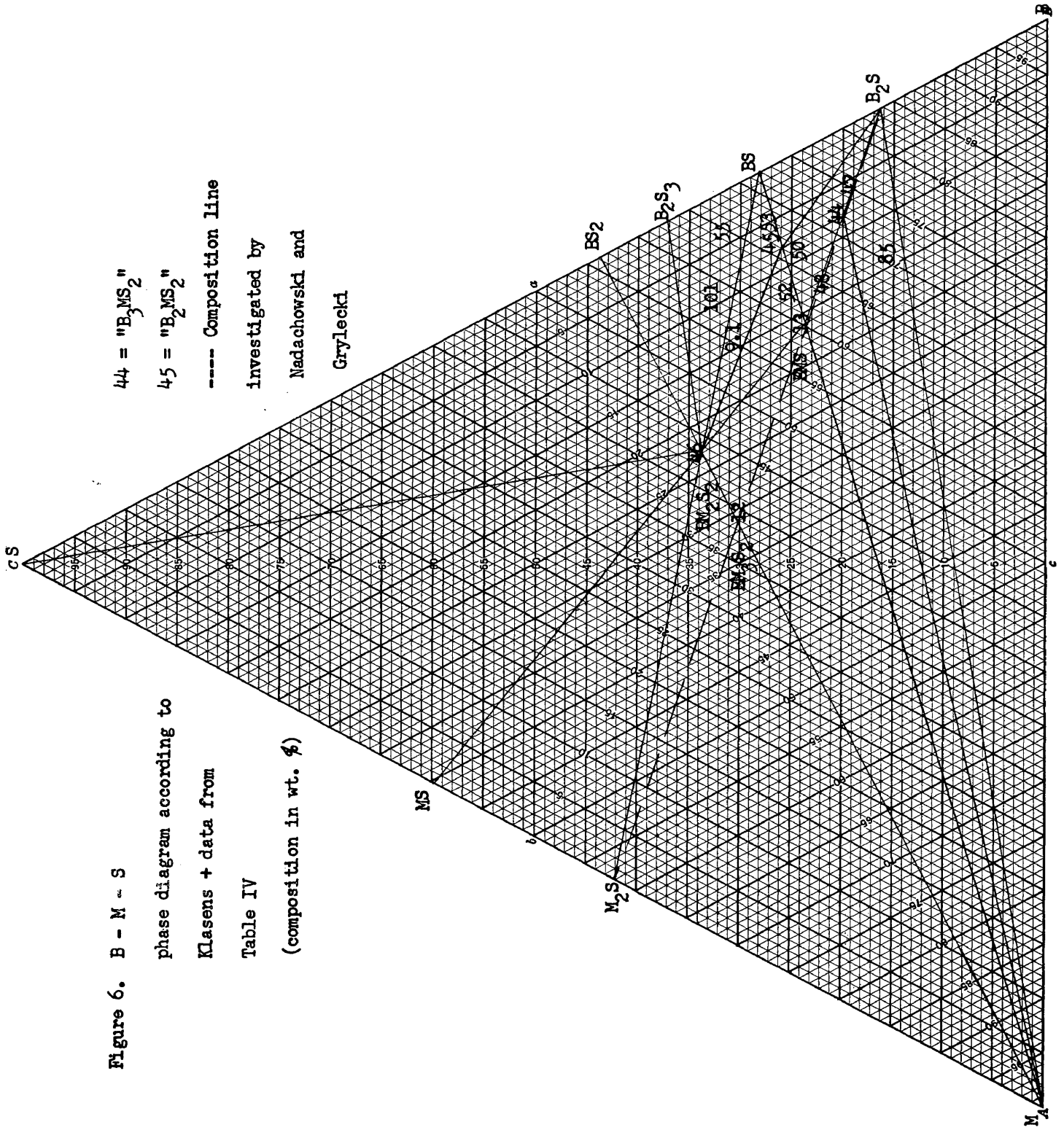
- a) EMS to BS_2 b) EMS to BS c) EMS to B_2S

An examination of the X-Ray pattern of samples No. 45 and 53 show a large amount of BS and a very small amount of EMS because pure BS is a very intense pattern compared to that of EMS. This is generally true of binary compounds compared to ternary compounds. Therefore, Klasens apparently confused the mixture of EMS and BS to such an extent as to term the mixture a new compound. When the X-Ray patterns of samples 13 (Table II), 52, 45, 53, and 6 are compared, it is seen that there is a regular progression from pure EMS (No. 13) to pure BS (No. 6). However the intensity of the lines of EMS drop approximately exponentially as the composition progresses toward BS. See Figure 8 for the X-Ray patterns.

There does not seem to be any reason that so-called B_3MS_2 should be reported as a new compound, since the X-Ray pattern for sample No. 44 very clearly shows a mixture of EMS and B_2S .

Figure 6. B - M - S
 phase diagram according to
 Klasens + data from
 Table IV
 (composition in wt. %)

44 = "B₃MS₂"
 45 = "B₂MS₂"
 ----- Composition line
 investigated by
 Nadachowski and
 Grylecki



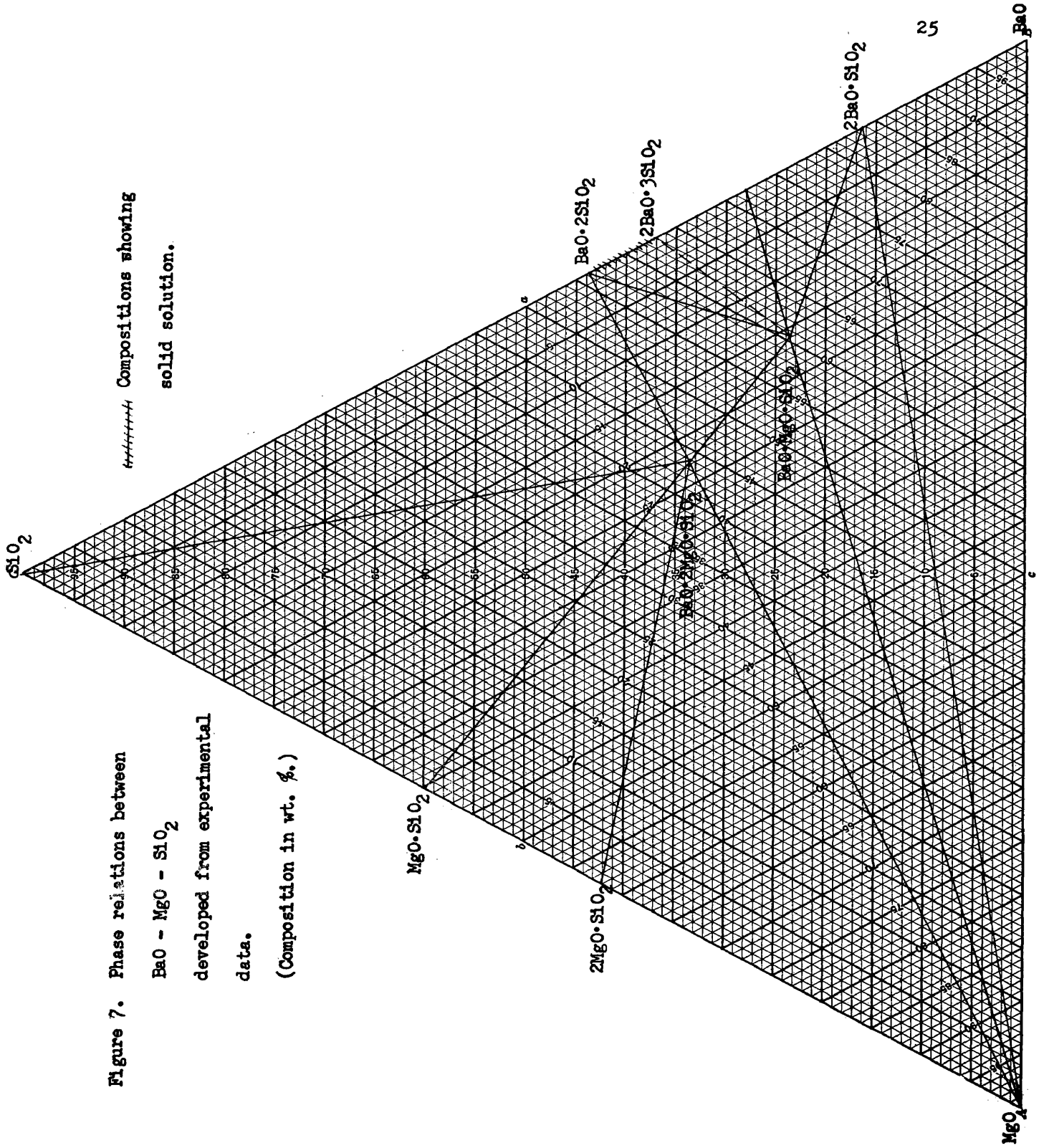


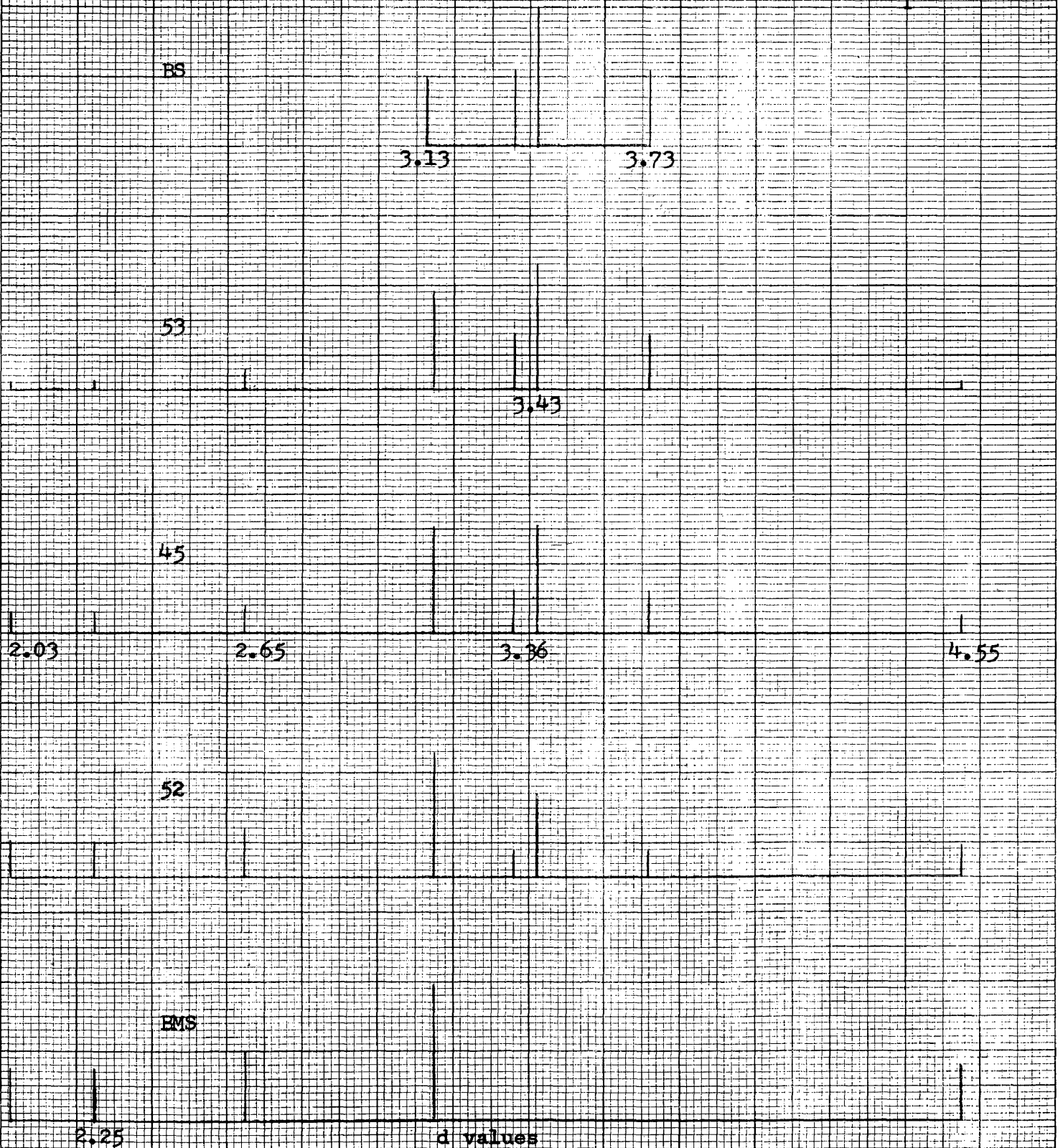
Figure 7. Phase relations between BaO - MgO - SiO₂ developed from experimental data. (Composition in wt. %.)

----- Compositions showing solid solution.

Figure 8: Comparison of X-Ray diffraction patterns

for composition between EMS and BS

Intensity = 50



The remainder of the diagram was verified by making the following compositions to identify compatible crystalline pairs of compounds.

Table V

Data for Developing Alkemade Lines

Composition No.	Compounds expected	% Composition			Firing Temperature	Crystals Identified
		BaO	MgO	SiO ₂		
88	S+EM ₂ S ₂	37.00	19.50	43.50	1210°C	S+EM ₂ S ₂
97	S+EM ₂ S ₂ +MS	24.40	26.53	49.07	1260°C	S+ " +MS
76	MS+EM ₂ S ₂	21.65	31.49	46.86	"	" + "
17	" + " +M ₂ S	19.44	35.43	45.13	"	M ₂ S+" + "
75	M ₂ S+EM ₂ S ₂	21.65	40.04	38.31	"	" + "
109	" + " +M	25.00	45.00	30.00	1280°C	" + " +M
84	M + "	19.44	65.33	15.23	1425°C	M + "
74	" + "	41.09	26.71	32.20	1260°C	" + "
93	EMS + M	30.22	57.94	11.84	1425°C	EMS+M
94	" + "	52.15	27.42	20.43	"	" +"
108	B ₂ S + M	41.81	50.00	8.19	1300°C	B ₂ S+M
95	" + " + B	50.80	42.50	6.70	"	" +"+BaCO ₃
107	" + " + "	90.00	5.00	5.00	"	" +"+ "
92	EM ₃ S ₂ +B ₂ MS ₂	52.26	19.64	28.10	1425°C	EM ₂ S ₂ +BMS
100	EM ₂ S ₂ +BS ₂ +S	24.40	6.42	69.18	1260°C	" +BS ₂ +S

Samples No. 88, 97, and 76 indicate that S, MS and EM_2S_2 are compatible phases and form an Alkemade triangle. Then samples No. 17 and 75 show that M_2S and EM_2S_2 are compatible to give an Alkemade line. Samples No. 109, 84, and 74 prove the Alkemade line M to EM_2S_2 . Samples No. 93 and 94 indicate that the Alkemade line between M and BMS is present. Samples No. 108, 95, and 107 show that the Alkemade triangle $M + B_2S + B$ is a compatible combination. The X-Ray pattern shows $BaCO_3$ to be present instead of BaO. This is to be expected since the samples were not heated above $1450^\circ C$ which is the temperature at which $BaCO_3$ loses its CO_2 to form BaO. When BaO is not a compatible phase the reaction between SiO_2 , MgO and $BaCO_3$ to form a binary or ternary compound is sufficient to eliminate the CO_2 from the $BaCO_3$ at a much lower temperature.

Sample No. 92 shows that EM_2S_2 and BMS are compatible, while sample No. 100 proves the point already made that the compounds S, EM_2S_2 and BS_2 are compatible also.

This leaves only the area BS_2 , B_2S_3 and BMS which has caused much confusion, since it is an area of solid solution.

Solid solution is rather common in non-metallic systems and the present one is no exception. The types of solid solution are interstitial and substitutional, the latter of which may be divided into random, ordered, or defect. Interstitial solid solution is indicated when the X-Ray pattern shows a shift in position of the lines to higher and to lower d-values on the same pattern. This means that the unit cell dimension is increasing in one direction and decreasing in another direction.

Random substitutional solid solution is accompanied by an increase or a decrease in the unit cell dimension, but both increase and decrease do not occur at the same time.

Ordered substitutional solid solution, in comparison, shows little or no shift in the lines but a large difference in intensity of the lines is noticed.

Defect substitutional solid solution is very rare in metal systems but rather common in oxide systems. It is characterized by a shift in position of the lines accompanied by the appearance of new lines, some of which may have high intensity and is also accompanied by changes in intensity of the lines of the original pattern. The following Table shows compositions which were made in the area which was liable to show solid solution, as such a condition was already reported for compositions between BS_2 and B_2S_3 .

Table VI

Data for Compounds in Solid Solution Area

Compo- sition No.	% Composition			Firing Tempe- rature	Crystals identified
	BaO	MgO	SiO ₂		
35	58.22	7.94	33.84	1250°C	BMS + (BS ₂ + B ₂ S ₃)ss*
36	61.70	7.94	30.36	"	" + " "
56	60.82	4.32	34.86	1260°C	" + " "

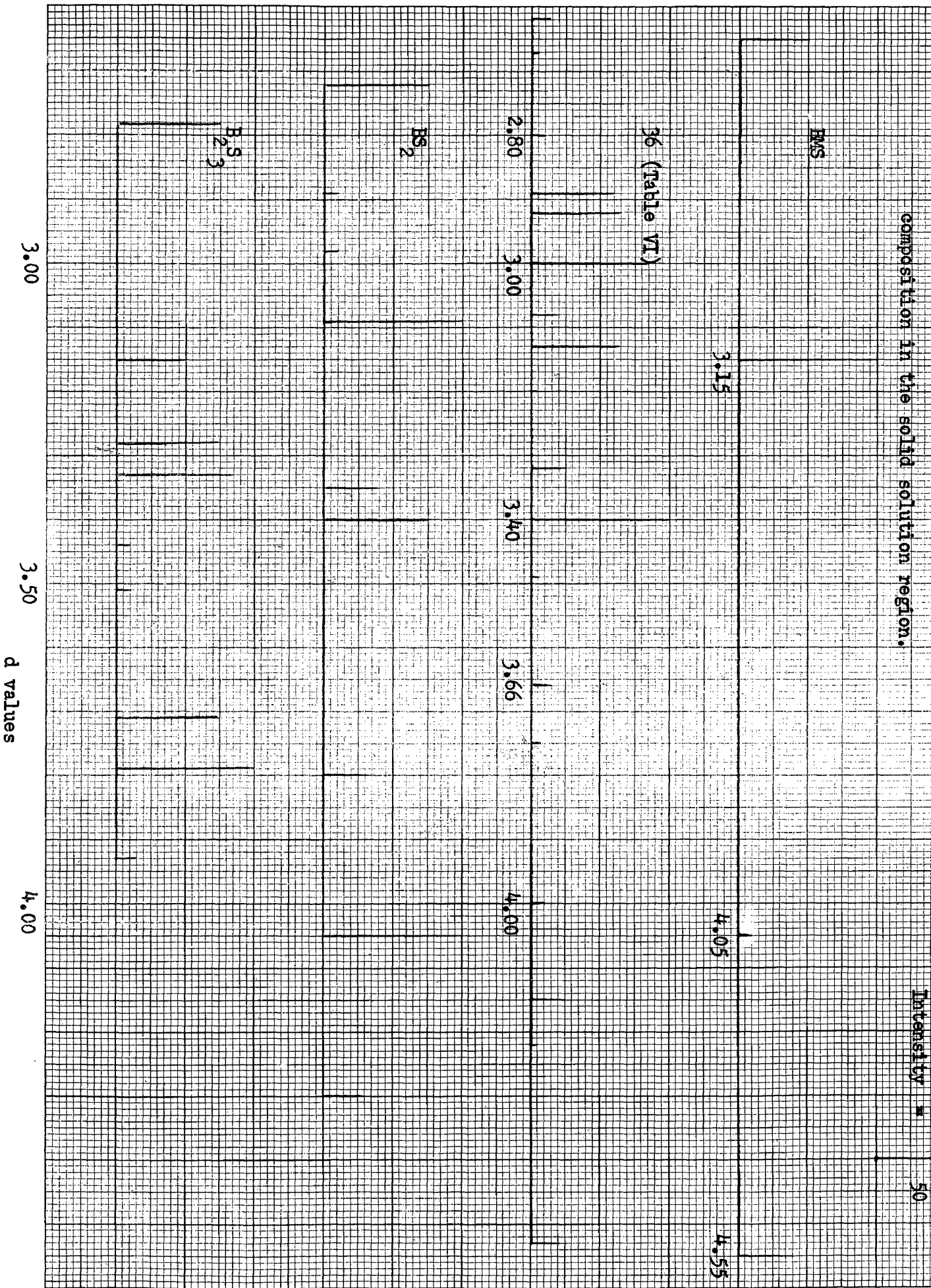
*ss = solid solution

Figure 9 shows the X-Ray diffraction patterns of sample No. 36, Sample No. 13 (EMS), Sample No. 5 (B_2S_3), and sample No. 4 (BS_2). This shows a shift in the position of the lines for BS_2 as well as a change in intensities. Also new lines are appearing, for instance the line at $d = 4.15$ A. U. ($2\theta = 21.38^\circ$). When this situation occurs it is very easy to assume that a new crystal has been formed. In this area, therefore, the data show that there is solid solution only between BS_2 and B_2S_3 while EMS is unaffected.

The Russians, Nadachowski and Grylecki, report a compound EM_3S_2 when they investigated compositions on a line between B_2S and M_2S . This line is shown on Figure 6, and where it crosses the Alkemade line between M and EM_2S_2 is the location of their compound " EM_3S_2 ". As pointed out previously (page 20) the X-Ray pattern for " EM_3S_2 " and for Klasens EM_2S_2 are very similar except for a shift in the lines for the so-called new compound.

Samples 74, 12, and 84 which are progressive changes in composition from EM_2S_2 to M, all show evidence of increasing M. The only way that the error can be accounted for in the Russians' work, is that they must have ignored the presence of the M lines. Also the Russians placed all their proof for the existence of EM_3S_2 on the presence on the X-Ray pattern of the line $d = 6.49$ A. U. which Klasens had not reported in his pattern for EM_2S_2 and which our experimental data always shows to be present when EM_2S_2 is present in a sample.

Figure 9: Comparison of X-Ray diffraction patterns for composition in the solid solution region.



Further work indicated in this system is to locate the eutectic compositions and temperatures. Once these are located the liquidus lines could be extended from the eutectic points. The third step is to then determine the contour of the liquidus surface by determining the isothermal lines.

SUMMARY

The experimental work for this thesis shows that in the ternary diagram for $\text{BaO} - \text{MgO} - \text{SiO}_2$, there are twenty-one Alkemade lines in the system. There are only two intermediate compounds in the system being EMS and EM_2S_2 . The Alkemade lines and triangles are as follows:

Binary Pairs of Crystals or Alkemade Lines	Ternary Groups of Crystals or Alkemade Triangles
1) $\text{S} - \text{MS}$	
2) $\text{S} - \text{EM}_2\text{S}_2$	
3) $\text{MS} - \text{EM}_2\text{S}_2$	1) $\text{S} - \text{MS} - \text{EM}_2\text{S}_2$
4) $\text{M}_2\text{S} - \text{EM}_2\text{S}_2$	
5) $\text{MS} - \text{M}_2\text{S}$	2) $\text{MS} - \text{M}_2\text{S} - \text{EM}_2\text{S}_2$
6) $\text{M} - \text{EM}_2\text{S}_2$	
7) $\text{M} - \text{M}_2\text{S}$	3) $\text{M} - \text{M}_2\text{S} - \text{EM}_2\text{S}_2$
8) $\text{M} - \text{EMS}$	
9) $\text{EM}_2\text{S}_2 - \text{EMS}$	4) $\text{M} - \text{EMS} - \text{EM}_2\text{S}_2$

- | | |
|----------------------------------|---------------------------------|
| 10) $M - B_2S$ | |
| 11) $B_2S - EMS$ | 5) $M - B_2S - EMS$ |
| 12) $M - B$ | |
| 13) $B - B_2S$ | 6) $M - B - B_2S$ |
| 14) $BS - B_2S$ | |
| 15) $BS - EMS$ | 7) $BS - B_2S - EMS$ |
| 16) $BS - B_2S_3$ | |
| 17) $EMS - B_2S_3$ | 8) $BS - EMS - B_2S_3$ |
| 18) $EMS - (B_2S_3 + BS_2)_{ss}$ | 9) $EMS - (B_2S_3 + BS_2)_{ss}$ |
| 19) $EMS - BS_2$ | |
| 20) $BS_2 - EM_2S_2$ | 10) $BS_2 - EMS - EM_2S_2$ |
| 21) $BS_2 - S$ | 11) $S - EM_2S_2 - BS_2$ |

ss = solid solution.

The existence of the solid solution between BS_2 and B_2S_3 was shown to be valid and also to be present as a phase in the area between $BS_2 + B_2S_3 + EMS$.

The experimental data prove that the two compounds, B_3MS_2 and B_2MS_2 , reported by Klasens do not exist. Also the compound, EM_3S_2 , reported by Nadachowski and Grylecki does not exist. Apparently these errors came about because of wrong interpretation of the X-Ray patterns and the use of an insufficient number of samples.

CONCLUSIONS

- 1) The phase system $\text{BaO} - \text{MgO} - \text{SiO}_2$ contains twenty-one Alkemade lines and eleven Alkemade triangles.
- 2) There are two intermediate compounds, $\text{BaO} \cdot 2\text{MgO} \cdot 2\text{SiO}_2$ and $\text{BaO} \cdot \text{MgO} \cdot \text{SiO}_2$ which occur in the system.
- 3) The compounds, $3\text{BaO} \cdot \text{MgO} \cdot 2\text{SiO}_2$, $2\text{BaO} \cdot \text{MgO} \cdot 2\text{SiO}_2$, and $\text{BaO} \cdot 3\text{MgO} \cdot 2\text{SiO}_2$ have been shown to be nonexistent.
- 4) Solid solution between $\text{BaO} \cdot 2\text{SiO}_2$ and $2\text{BaO} \cdot 3\text{SiO}_2$ has been verified by the X-Ray patterns.

APPENDIX A

In this Appendix A, the X-Ray patterns were obtained from the A.S.T.M. card file unless otherwise noted.

1) BaCO_3 (Witherite)

<u>d. A. U.</u>	<u>Int.</u>	<u>2θ. deg.</u>
4.56	9	19.45
4.45	4	19.93
3.72	100	23.90
3.68	53	24.16
3.215	15	27.72
3.025	4	29.50
2.749	3	32.54
2.656	11	33.72
2.628	24	34.08
2.590	23	34.60
2.281	6	39.48
2.226	2	40.48
2.150	28	41.98
2.104	12	42.94
2.048	10	44.18
2.019	21	44.86
1.940	15	46.78

2) BaO

<u>d. A.U.</u>	<u>Int.</u>	<u>2θ. deg.</u>
3.20	100	27.86
2.75	88	32.54
1.95	75	46.54
1.66	50	55.30
1.59	25	57.94
1.38	10	67.86

3) $\text{BaO} \cdot \text{SiO}_2$

<u>d. A.U.</u>	<u>Int.</u>	<u>2θ. deg.</u>
5.19	19	17.07
4.20	10	21.14
3.73	55	23.84
3.58	17	24.84
3.43	100	25.96
3.36	57	26.50
3.13	50	28.50
2.84	32	31.48
2.75	18	32.54
2.71	23	33.02
2.59	9	34.60
2.36	31	38.10
2.30	35	39.12
2.24	31	40.24
2.19	5	41.18
2.14	11	42.20
2.09	19	43.24
2.08	36	43.46
2.04	45	44.36
2.01	7	45.06
1.977	7	45.86
1.896	32	47.94
1.852	16	49.14
1.795	9	50.82
1.781	9	51.24
1.761	12	51.86
1.737	12	52.64
1.698	33	53.94

4) α -BaO \cdot 2SiO₂ (Sanbornite)

<u>d, A.U.</u>	<u>Int.</u>	<u>2θ, deg.</u>
6.90	10	12.82
5.60	10	15.82
4.75	10	18.66
4.05	100	21.92
3.85	15	23.08
3.55	50	25.06
3.35	40	26.58
3.27	35	27.24
3.17	75	28.12
2.88	35	31.02
2.78	45	32.16
2.61	25	34.32
2.51	20	35.74
2.41	5	37.28
2.35	35	38.26
2.26	60	39.84
2.22	80	40.60
2.16	25	41.78
2.07	40	43.68
2.04	35	44.36
2.00	15	45.30
1.95	20	46.52
1.92	40	47.30
1.88	40	48.36
1.83	20	49.78
1.79	30	50.96
1.68	10	54.58
1.60	55	57.56
1.48	20	62.72

4) β -BaO \cdot 2SiO $_2$ (Sanbornite)

<u>d, A.U.</u>	<u>Int.</u>	<u>2θ, deg.</u>
6.80	20	13.00
6.4	5	13.82
5.8	5	15.26
5.5	5	15.96
5.0	30	17.72
4.3	30	20.64
4.0	95	22.20
3.8	30	23.38
3.40	75	26.18
3.32	95	26.82
3.25	35	27.42
3.09	100	28.86
2.98	10	29.96
2.89	10	30.90
2.72	75	32.90
2.58	25	34.74
2.54	5	35.30
2.50	5	35.88
2.40	10	37.44
2.32	20	38.78
2.23	60	40.40
2.19	25	41.18
2.16	40	41.78
2.13	60	42.40
2.11	20	42.82
2.03	30	44.60
1.99	20	45.54
1.92	30	47.30
1.915	25	47.44
1.855	25	49.06
1.795	35	50.82
1.69	35	54.22

5) $2\text{BaO} \cdot \text{SiO}_2$

<u>d. A.U.</u>	<u>Int.</u>	<u>2θ. deg.</u>
4.23	20	20.98
3.43	63	25.96
3.17	16	28.12
3.11	14	28.68
3.03	100	29.46
2.95	95	30.28
2.91	82	30.70
2.69	10	33.28
2.56	8	35.02
2.53	14	35.44
2.44	36	36.80
2.40	25	37.44
2.30	6	39.14
2.24	27	40.22
2.12	24	42.60
2.10	36	43.04
2.02	8	44.84
1.975	22	45.90
1.909	17	47.58
1.867	22	48.73
1.788	10	51.04
1.762	33	51.84
1.710	47	53.54
1.686	11	54.36
1.659	7	55.32
1.645	8	55.84
1.598	5	57.62

6) $2\text{BaO} \cdot 3\text{SiO}_2$

<u>d, A.U.</u>	<u>Int.</u>	<u>2θ, deg.</u>
7.11	15	12.44
6.06	11	14.60
3.93	13	22.60
3.79	100	23.44
3.71	75	23.96
3.51	10	25.36
3.44	10	25.88
3.33	87	26.74
3.28	76	27.16
3.15	48	28.30
2.78	74	32.16
2.61	8	34.32
2.41	8	37.28
2.36	35	38.10
2.28	45	39.48
2.23	32	40.40
2.21	24	40.78
2.14	60	42.20
2.09	22	43.26
2.04	12	44.36
1.981	20	45.76
1.918	14	47.36
1.881	8	48.34
1.825	14	49.92
1.811	17	50.34
1.789	25	51.00
1.760	11	51.90
1.745	11	52.38
1.654	22	55.50
1.636	10	56.16

7) $BaO \cdot MgO \cdot SiO_2$

Nadachowski and Grylecki pattern

Klasens pattern

<u>d, A.U.</u>	<u>Int.*</u>	<u>2θ, deg.</u>	<u>d, A.U.</u>	<u>Int.</u>	<u>2θ, deg.</u>
4.61	m	19.24	4.55	40	19.50
4.03	s.s	22.04	4.05	10	21.92
3.15	m.st	28.30	3.15	100	28.30
2.64	m	33.92	2.65	50	33.80
2.26	m	39.86	2.53	10	35.44
2.19	s	41.18	2.47	5	36.34
2.02	m	44.84	2.25	40	40.04
1.98	s	45.78	2.18	15	41.38
1.72	s.s	53.20	2.03	40	44.60
1.68	s	54.58	1.96	25	46.28
1.60	m	57.56	1.72	15	53.20
1.58	s	58.36	1.68	20	54.58
1.52	s	60.90	1.63	5	56.40
1.385	s.s	67.58	1.60	40	57.56
			1.58	15	58.36
			1.52	20	60.90
			1.385	10	67.58

* s.s: very weak

s: weak

m: medium

m.st: medium strong

st: strong

8) $\text{BaO} \cdot 2\text{MgO} \cdot 2\text{SiO}_2$

<u>d. A.U.</u>	<u>Int.</u>	<u>2θ. deg.</u>
4.60	20	19.28
3.60	10	24.70
3.40	20	26.18
3.20	100	27.86
3.15	65	28.30
3.00	45	29.76
2.88	15	31.02
2.85	20	31.36
2.70	5	33.16
2.62	5	34.20
2.49	30	36.04
2.35	25	38.26
2.32	15	38.78
2.25	50	40.04
2.14	15	42.20
2.10	10	43.04
2.00	15	45.30
1.95	30	46.52
1.93	35	47.04
1.84	10	49.50
1.75	15	52.22
1.72	15	53.20
1.69	15	54.22
1.65	15	55.66
1.61	10	57.16
1.56	20	59.18
1.51	15	61.34
1.49	5	62.26

9) $\text{BaO} \cdot 3\text{MgO} \cdot 2\text{SiO}_2$ **

<u>d, A.U.</u>	<u>Int.*</u>	<u>2θ, deg.</u>
6.49	s.s	13.64
4.61	s	19.24
3.24	m	27.50
3.15	s	28.30
3.05	s	29.26
2.87	s.s	31.14
2.61	s.s	34.32
2.50	s	35.88
2.26	s	39.86
2.15	s.s	41.98
2.11	s.s	42.82
1.94	s	45.06
1.89	s.s	48.10
1.79	s.s	50.96
1.72	s.s	53.20
1.70	s.s	53.88
1.65	s.s	55.66
1.52	s.s	59.18

* See page 45.

** Pattern obtained from work by Nadachowski and Grylecki (13).

10) $2\text{BaO} \cdot \text{MgO} \cdot 2\text{SiO}_2$

<u>d, A.U.</u>	<u>Int.</u>	<u>2θ, deg.</u>
5.40	5	16.40
3.93	40	22.60
3.45	20	25.80
3.17	100	28.12
3.02	10	29.56
2.92	55	30.60
2.86	20	31.24
2.72	25	32.90
2.54	10	35.30
2.39	20	37.60
2.36	10	38.10
2.21	20	40.80
2.12	10	42.60
2.08	25	43.46
2.06	20	43.92
2.02	5	44.82
1.94	45	46.78
1.91	20	47.56
1.85	20	49.20
1.79	10	50.98
1.74	10	52.54
1.70	30	53.88
1.65	10	55.66
1.595	5	57.74
1.555	15	59.38
1.55	5	59.60
1.495	15	62.02
1.485	10	62.48
1.460	10	63.68

11) $3\text{BaO}\cdot\text{MgO}\cdot 2\text{SiO}_2$

<u>d, A.U.</u>	<u>Int.</u>	<u>2θ, deg.</u>
4.05	70	21.92
3.41	5	26.10
3.16	10	28.22
3.02	5	29.56
2.93	95	30.48
2.81	100	31.82
2.43	35	36.96
2.31	55	38.96
2.03	65	44.60
1.84	40	49.50
1.78	25	51.28
1.71	20	53.54
1.64	50	56.02
1.63	30	56.40
1.53	10	60.46
1.46	20	63.68
1.405	30	66.48
1.395	15	67.02

12) MgCO_3 (Magnesite)

<u>d, A.U.</u>	<u>Int.</u>	<u>2θ, deg.</u>
3.53	20	25.20
2.74	100	32.66
2.50	60	35.90
2.31	40	38.96
2.10	80	43.04
1.93	60	47.04
1.77	40	51.60
1.70	90	53.88
1.51	40	61.34
1.48	50	62.72
1.40	60	66.76
1.37	20	68.42

13) MgO (Periclase)

<u>d, A.U.</u>	<u>Int.</u>	<u>2θ, deg.</u>
2.431	10	36.94
2.106	100	42.90
1.489	52	62.30
1.270	4	
1.216	12	
1.05333	5	
0.9665	2	
.9419	17	
.8600	15	
.8109	3	

14) $\text{MgO} \cdot \text{SiO}_2$ (Clinoenstatite)

<u>d, A.U.</u>	<u>Int.</u>	<u>2θ, deg.</u>
4.42	10	20.06
4.32	10	20.54
3.28	60	27.16
3.16	60	28.22
2.97	90	30.06
2.87	100	31.14
2.54	40	35.30
2.52	40	35.60
2.44	40	36.80
2.42	20	37.12
2.36	10	38.10
2.18	10	41.38
2.10	60	43.04
2.08	10	43.46
2.00	10	45.30
1.98	10	45.78
1.96	10	46.28
1.93	10	47.04
1.78	20	51.28
1.73	20	52.88
1.72	20	53.20
1.64	10	56.02
1.60	80	57.56
1.58	10	58.36
1.52	40	60.90
1.48	20	62.72
1.46	40	63.68
1.39	10	67.30

15) $2\text{MgO}\cdot\text{SiO}_2$ (Forsterite)

<u>d, A.U.</u>	<u>Int.</u>	<u>2θ, deg.</u>
5.11	26	17.34
3.88	69	22.90
3.73	25	23.84
3.487	21	25.52
3.000	17	29.76
2.768	53	32.32
2.513	73	35.70
2.458	100	36.52
2.348	9	38.30
2.316	9	38.86
2.268	59	39.70
2.250	33	40.04
2.161	15	41.76
2.034	5	44.50
1.945	4	46.66
1.878	5	48.42
1.811	2	50.34
1.792	3	50.92
1.748	60	52.30
1.670	13	54.94
1.636	12	56.18
1.618	15	56.86
1.589	2	58.00
1.572	10	58.68
1.531	1	60.40
1.514	10	61.16
1.497	27	61.94
1.479	30	62.76

16) SiO₂ (α-quartz)

<u>d, A.U.</u>	<u>Int.</u>	<u>2θ, deg.</u>
4.26	35	20.83
3.343	100	26.64
2.458	12	36.52
2.282	12	39.46
2.237	6	40.28
2.128	9	42.44
1.980	6	45.80
1.817	17	50.16
1.801	1	50.64
1.672	7	54.86
1.659	3	55.33
1.608	1	57.24
1.541	15	59.98
1.453	3	64.02

17) SiO₂ (α -cristobalite)

<u>d, A.U.</u>	<u>Int.</u>	<u>2θ, deg.</u>
3.99	100	22.26
3.19	80	27.94
2.94	40	30.38
2.82	40	31.70
2.50	60	35.90
2.11	40	42.82
2.02	40	44.82
1.93	40	47.04
1.86	40	48.92
1.78	20	51.28
1.69	40	54.22
1.60	60	57.56
1.54	40	60.02
1.49	60	62.24
1.43	40	65.18

18) SiO_2 (α -tridymite)

<u>d, A.U.</u>	<u>Int.</u>	<u>2θ, deg.</u>
4.30	100	20.64
4.08	33	21.76
3.81	67	23.32
3.43	1	25.96
3.21	1	27.76
2.96	17	30.16
2.80	3	31.94
2.49	27	36.04
2.31	11	38.96
2.08	5	43.46
1.84	3	49.50
1.69	8	54.22
1.64	4	56.02
1.60	4	57.56
1.53	5	60.46
1.44	3	64.68
1.40	7	66.76

BIBLIOGRAPHY

1. Bowen, N. L. and Anderson, O. "The binary system MgO - SiO₂." Am. J. Sci. (4), 37, 488 (1914).
2. Grieg, J. W. "Immiscibility in silicate melts." Am. J. Sci. (5), 13, 15, 133-54 (1927).
3. Swanson and Tatge. "Standard X-Ray diffraction powder patterns." NBS circular 539, I, 37-8 (1953).
4. Index to the X-Ray Powder Data File. ASTM Special Technical Publication 48-2 (1962).
5. Bragg and Brown, Z. Krist 63, 538 (1926).
6. Swanson and Fuyat. "Standard X-Ray diffraction patterns. NBS Circular 539, III, 24-6 (1959).
7. Clark, C. B., "X-Ray diffraction data for compounds in the system CaO - MgO - SiO₂." J. Am. Ceram. Soc. 29, 25 (1946).
8. Wartenberg, H. von and Prophet, E. "Schmelzdiagramme höchstfeuerfester oxyde, V. Systeme mit MgO." Part V, Z. anorg. U. allgem. Chem. 208, 378 (1932).
9. Wyckoff, "The crystal structures of the compounds RX." The Structure of Crystals, page 224 (1963).
10. Eskola, P. "The silicates of strontium and barium." Am. J. Sci. 5th, ser. 4, 345 (1922).
11. Grieg, J. W. "The system BaO - SiO₂." Am. J. Sci., 5th ser. 13 27, (1927).

12. Klasens, H. A., Hoekstra, A. H., and Cox, A.P.M. "Ultra-violet fluorescence of some ternary silicates activated with lead." *J. Electrochem. Soc.* 104, 93-99 (1957).
13. Nadachowski, F. and Grylecki, M. "Phasen - Gleichgewichte im system $2\text{BaO}\cdot\text{SiO}_2 - 2\text{CaO}\cdot\text{SiO}_2 - 2\text{MgO}\cdot\text{SiO}_2$." *Silikattechn* 10, 77-80 (1959).
14. Yasuno, F. "Equilibrium diagram of the area sanbornite - forsterite - silica in the ternary system of $\text{MgO} - \text{BaO} - \text{SiO}_2$, studies on the deterioration phenomenon of steatite bodies, III." *J. Cer. Assoc. Japan*, 67, 403-19 (1959).
15. Turner, C. H. "Approximate composition of the lowest fusing mixture of barium oxide, magnesium oxide, and silica." *J. Amer. Cer. Soc.* 17, 14-15 (1934).

VITA

The author was born in Polatli, Ankara, Turkey on November 19, 1935. After attending the Technical University of Istanbul he received the degree of Master of Science in Mining Engineering in 1961. At that time he became an Instructor in the Metallurgy Department of I.T.U. During the summers he worked at the Rabak Electrolytic Copper Refinery in the pyrometallurgical department. During the school year he took courses in the Metallurgy Department preparatory to working on his Doctor's degree. In July of 1963 he came to the Colorado School of Mines to work on the Master of Science degree in Metallurgical Engineering. During this time he was supported by the Agency for International Development, United States Department of State (AID) and by the Turkish Government.